Biomed Microdevices (2006) 8: 109–118
DOI 10.1007/s10544-006-7706-6

A parallel-gradient microfluidic chamber for quantitative analysis of breast cancer cell chemotaxis

Wajeeh Saadi · Shur-Jen Wang · Francis Lin · Noo Li Jeon

Abstract Growth factor-induced chemotaxis of cancer cells is believed to play a critical role in metastasis, directing the spread of cancer from the primary tumor to secondary sites in the body. Understanding the mechanistic and quantitative behavior of cancer cell migration in growth factor gradients would greatly help in future treatment of metastatic cancers. Using a novel microfluidic chemotaxis chamber capable of simultaneously generating multiple growth factor gradients, we examined the migration of the human metastatic breast cancer cell line MDA-MB-231 in various conditions. First, we quantified and compared the migration in two gradients of epidermal growth factor (EGF) spanning different concentrations: 0–50 ng/ml and 0.1–6 ng/ml. Cells showed a stronger response in the 0–50 ng/ml gradient. However, the fact that even a shallow gradient of EGF can induce chemotaxis, and that EGF can direct migration over a large dynamic range of gradients, confirms the potency of EGF as a chemoattractant. Second, we investigated the effect of antibody against the EGF receptor (EGFR) on MDA-MB-231 chemotaxis. Quantitative analysis indicated that anti-EGFR antibody impaired both motility and directional orientation (CI = 0.03, speed = 0.71 μm/min), indicating that cell motility was induced by the activation of EGFR. The ability to compare, in terms of quantitative parameters, the effects of different pharmaceutical inhibitors, as well as subtle differences in experimental conditions, will aid in our understanding of mechanisms that drive metastasis. The microfluidic chamber described in this work will provide a platform for cell-based assays that can be used to compare the effectiveness of different pharmaceutical compounds targeting cell migration and metastasis.

W. Saadi · S.-J. Wang · N. L. Jeon (✉)
Department of Biomedical Engineering, 3120 Natural Sciences II, University of California, Irvine, Irvine, CA, 92697
e-mail: njeon@uci.edu

F. Lin
Department of Biomedical Engineering, 3120 Natural Sciences II, University of California, Irvine, Irvine, CA, 92697; Department of Physics and Astronomy, University of California at Irvine, Irvine, CA, 92697, U.S.A

Introduction

Cell motility plays an important role in many biological processes, including inflammation (Yang et al., 1999), wound healing (Maheshwari et al., 1999), and cancer metastasis (Condeelis et al., 2001; Kassis et al., 2001; Wells et al., 2002). Of particular importance in these processes is chemotaxis: directed motility towards increasing concentrations of soluble factors. The study of cell motility and chemotaxis, like any experimental system, is often defined by the assays employed (Wells, 2000). One of the most commonly used assays is the Boyden chamber (also called transfilter or transwell assay), which measures motility as the number of cells that migrate across a filter between two compartments containing soluble factors (Wilkinson, 1998). In spite of its popularity, this method does not allow visualization of the actual migration paths, providing only an endpoint measurement. In addition, comparisons of cells with different sizes or different abilities to deform may be inaccurate, since cells have to deform in order to migrate through the pores and cross the filter (Wells, 2000). Surface assays (such as wound-healing, colony scattering, and under-agarose assays) overcome the deformability problem by allowing cells to migrate on a flat surface, but most are still endpoint assays and cannot always

be utilized to study chemotaxis (Wells, 2000). Visual assay systems allow the details of the motility process to be studied, and allow chemotaxis to be observed, usually in response to pipette tips containing soluble factors, but are generally low throughput, best suited for single-cell measurements (Wells, 2000).

In addition, a major deficiency of most conventional assays is their inability to maintain stable concentration gradients over time (Dertinger et al., 2001; Jeon et al., 2002). Quantitative descriptions of gradient conditions produced by these methods require complicated mathematical modeling (Jeon et al., 2002). Consequently, the relationships between various chemical signals and the resulting chemotactic responses of different cells have been difficult to characterize rigorously. Advances in soft lithography and microfluidics enabled the development of chemotaxis chambers that can generate precise, stable concentration gradients, and allow real-time observation of migrating cells (Jeon et al., 2000; Dertinger et al., 2001). This method was used to investigate the migration of neutrophils (Jeon et al., 2002) and breast cancer cells (Wang et al.) in IL-8 and epidermal growth factor (EGF) gradients, respectively. In both cases, the chemotaxis chambers were used to produce and maintain precise and stable gradient conditions that allowed quantitative characterization of directed cell migration to be performed.

In order for the microfluidic assay to be broadly useful in biology, it should easily lend itself to comparative measurements of chemotaxis in different conditions. This requires controls to be performed alongside of experiments, and different experimental conditions to be carried out in parallel. To this end, we developed a parallel-gradient microfluidic chemotaxis chamber that can generate soluble gradients of growth factors side by side, allowing two or more experiments to be carried out simultaneously using one imaging setup. With this capability, we can quantitatively analyze chemotactic responses in different conditions with a high degree of control, allowing us to detect subtle differences with exquisite detail. Using this approach, we first compared the chemotactic response of the cancer cells in two different concentration gradients of EGF; these gradients have the same profile but span different ranges of concentration (0–50 ng/ml and 0.1–6 ng/ml). Both gradients induced chemotaxis, but the response was stronger in the 0–50 ng/ml gradient. This demonstrates that EGF is a potent chemoattractant capable of inducing chemotaxis over a wide range of gradients. We then verified the specificity of the induced chemotactic response using an antibody that blocks the EGF receptor (EGFR). Both motility and directional sensing were lost when EGFR was blocked. These findings have relevance to the metastatic process and therapeutic efforts, and hint at the wealth of information that can be obtained from studies of cancer cell chemotaxis.

Methods

Cell culture

Leibovitz's L-15 medium, penicillin/streptomycin, trypsin/EDTA, Cell dissociation buffer, and fetal bovine serum (FBS) were purchased from GIBCO (Carlsbad, CA). Recombinant human EGF, bovine serum albumin, and human collagen type IV were purchased from Sigma (St Louis, MO). Mouse monoclonal neutralizing anti-EGFR antibody was purchased from Upstate Biotechnology (Lake Placid, NY). The human metastatic breast cancer cell line, MDA-MB-231, was obtained from The American Type Culture Collection (ATCC, Manassas, VA) and routinely passaged in L-15 medium supplemented with 10% FBS and penicillin/streptomycin.

Device fabrication

The microfluidic gradient generator was fabricated in poly (dimethylsiloxane) (PDMS) using soft lithography and rapid prototyping (Whitesides et al., 2001). Briefly, a transparency mask with a minimum feature size of $\sim$30 μm was printed using a high-resolution printer (Page One, Irvine, CA) from a CAD file (Freehand, Macromedia, CA). The mask was used in 1:1 contact photolithography of SU-8 photoresist (MicroChem, MA) to generate a negative "master" consisting of 100 μm high patterned photoresist on a Si wafer (Silicon Inc., Boise, ID). Positive replicas with embossed channels were fabricated by molding PDMS (Sylgard 184, Dow Corning, Midland, MI) against the master. The cured PDMS was peeled off the master, and holes were punched with a sharpened needle for fluidic interconnects. The PDMS was sealed against a glass slide upon treating both with an air-plasma (Plasma cleaner Model PDC-001, Harrick Plasma, Ithaca, NY), forming a covalent bond and completing the microfluidic network. All channels were made of PDMS with glass bottoms.

Microfluidics

Prior to the cell migration experiment, the 400-μm wide migration channel was coated with 2 μg/ml collagen type IV at room temperature for 30 min. The collagen was then removed and the channel was washed twice with distilled water and blocked with 2% BSA at 37°C for 2 hrs or at 4°C overnight. Polyethylene tubing (PE-20, Becton Dickinson, Sparks, MD) was inserted into the inlets and connected to syringe pumps (model 50300, Kloehn Ltd., Las Vegas, NV) to infuse the solutions through the microfluidic device. The solutions were made up of 0.2% BSA in L-15 medium (0.2% BSA/L-15), with or without growth factor. To visualize the concentration gradient profile of EGF (MW = 6 kDa), 5 μM FITC-dextran

(Sigma) with a molecular weight of 10 kDa was added to the EGF solutions. A control experiment with FITC-dextran indicated no effect on migration.

Cell migration assay

MDA-MB-231 cells were removed from the culture flask using cell dissociation buffer, washed with 0.2% BSA/L-15, centrifuged down, resuspended in 0.2% BSA/L-15, and filtered through a 40-μm filter to obtain a suspension of single cells. For the anti-EGFR experiments, cells were counted after they were taken out of the flask, centrifuged down, and resuspended in anti-EGFR solution (in 0.2% BSA/L-15) at a density of 1×10^6 cells/ml prior to filtration. Antibody-treated cells, along with untreated cells, were then incubated on a rotator for 1 hr at room temperature. The cells were loaded into the microfluidic device from the cell port using a micropipette. The flow inside the device was slowed down or stopped to facilitate the attachment of cells to the bottom of the migration channels. Once the cells attached, a flow rate of 1 μl/min (equivalent to a linear speed of 4.2×10^{-2} cm/s) was applied. For the anti-EGFR experiments, anti-EGFR was added to the solutions flowing over the antibody-treated cells.

Time-lapse differential interference contrast (DIC) images of migrating cells were obtained using an inverted microscope (Nikon, Meville, NY) with a 10X objective. The microscope stage was enclosed in a temperature-controlled box maintained at 37°C. Images were acquired with a CCD camera (CoolSNAP cf, Photometrics, Tucson, AZ) at 2 min intervals for 3 hrs. A computer-controlled motorized stage was used to image multiple positions along the migration channel.

Data analysis

Time-lapse images of cells were tracked and analyzed using MetaMorph (Molecular Devices, Sunnyvale, CA). Raw tracking data for each cell were analyzed with a spreadsheet to calculate various migration parameters [(1) net cell displacement (straight length of cell displacement between starting and final positions), (2) total distance (sum of straight-line segments that a cell travels between consecutive images), (3) net displacement towards gradient, (4) speed (total distance divided by time), (5) migration angle (angle of the net cell displacement vector, measured clockwise from the positive y direction), and (6) chemotactic index (CI, net displacement towards gradient divided by total distance)]. Migration angles are defined with respect to the gradient direction (0° and 180° = net displacement perpendicular to gradient direction, 90° = net displacement completely in the gradient direction, 270° = net displacement completely opposite of gradient direction). CI is a measure of how much of the total movement is directed towards the gradient, ranging from -1 (cell moves completely opposite of gradient direction) through 0 (cell moves perpendicular to gradient direction) to 1 (cell moves completely in the gradient direction).

Statistical analysis of migration angles was performed using Oriana for Windows (Kovach Computing Services, Wales, UK) to examine the directionality of the chemotactic response. Migration angles were summarized in a direction plot, which is a rose diagram showing the distribution of angles grouped in 10° intervals, with the radius of each wedge indicating cell number. The Rayleigh test for circular uniformity was applied, with a significance level of 0.01. When there was significant directionality, the mean angle and the 95% confidence interval were calculated. A Modified Rayleigh test was also applied, in order to test whether deviations from the gradient direction were significant (Zar, 1996).

The non-linear polynomial gradient [Fig. 1(a)] used in this paper was divided into two regions: a shallow region (positions 0 to 160 μm on the x axis), where the concentration of ligand remains very low; and a steep region (positions 160 to 400 μm on the x axis), where the concentration of ligand increases very rapidly. Cells that were predominantly migrating in the shallow region of the gradient were excluded from the analysis. For each experimental condition, a minimum of 50 cells was analyzed.

Results

Generation of parallel gradients

The microfluidic chemotaxis chamber is comprised of a gradient-generating network of channels that merge into the migration channel near the outlet (Fig. 1). The design shown in [Fig. 1(a)] produces a nonlinear polynomial gradient similar in shape to that produced by diffusion from a micropipette, but is stable over time. The gradient profile for EGF is indirectly visualized using FITC-dextran, added to the EGF solution. A fluorescence micrograph and a graph showing the gradient profile are shown below the schematic. If a chamber consists of two adjacent networks that merge into one migration channel, two gradients are produced in parallel [Fig. 1(b)]. Since the two networks are mirror images of each other, the two gradients are identical in shape but opposite in direction. Figure 1(c) represents the same parallel-gradient design, with the addition of a physical barrier between the two gradients.

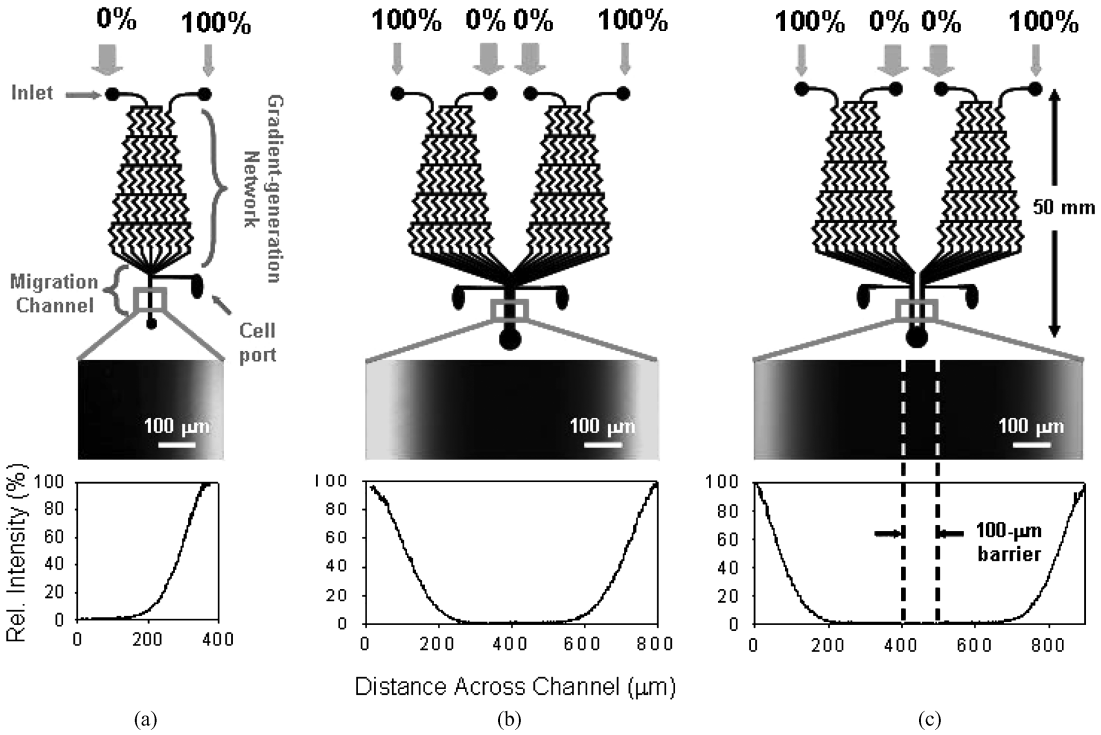

Fig. 1 Schematic diagrams of the microfluidic chemotaxis chambers. (a) A single-gradient chemotaxis chamber that produces a polynomial gradient. The gradient was visualized by injecting media with 0% and 100% FITC-dextran from the inlets, with a volumetric flow rate ratio of 4:1 respectively. A fluorescence (pseudo colored) image of the migration channel and a corresponding intensity profile are shown at the bottom. (b) A parallel-gradient chemotaxis chamber producing two opposite gradients side by side. (c) A parallel-gradient chemotaxis chamber with a 100-μm barrier in the middle of the migration channel

Shallow EGF concentration gradient can induce chemotaxis of metastatic breast cancer cells

EGF has been shown to induce chemotaxis of a variety of cancer cells, including breast cancer cells (Bailly et al., 1998; Bredin et al., 1999; Price et al., 1999; Wyckoff et al., 2000). We have previously reported, using a microfluidic chemotaxis chamber, that the shape of EGF gradient determines whether the migration is directed or random (Wang et al.). We found that nonlinear polynomial gradients of EGF induced chemotaxis of MDA-MB-231, while linear gradients resulted in random migration. Under our experimental conditions (Wang et al.), a polynomial gradient of 0–50 ng/ml EGF induced the most pronounced chemotactic response.

To investigate migration in a shallower EGF gradient, we used the parallel-gradient chamber without barrier (Figure 1b). We tested the migration of breast cancer cells in a 0.1–6 ng/ml polynomial EGF gradient alongside a 0–50 ng/ml EGF gradient (Fig. 2). In 0–50 ng/ml EGF, cells moved chemotactically, similar to previous findings (Wang et al.) with an average CI of 0.29. Moreover, the Rayleigh test showed significant unimodal clustering of cell trajectories, with a mean angle of 87.4°, in close alignment with the gradient direction [Fig. 2(b)]. Cells in the 0.1–6 ng/ml EGF gradient had a wider distribution of trajectories and a smaller average CI (0.10), but still exhibited preferential directional orientation, with a mean angle of 53.9° [Fig. 2(c)]. A modified Rayleigh test (Zar, 1996) showed that this angle does not significantly deviate from the gradient direction, confirming that the 0.1–6 ng/ml EGF gradient can induce chemotaxis.

Anti-EGFR inhibits EGF-induced chemotaxis in microfluidic chamber

The effect of EGFR-blocking antibody on MDA-MD-231 chemotaxis in EGF gradients was examined using the parallel-gradient chamber, with the addition of a barrier [Fig. 1(c)]. Migration of cells pretreated with antibody was examined in 0–50 ng/ml EGF alongside untreated control cells. Untreated cells clearly exhibited polarized morphology, characterized by a flat, fan-shaped lamellipod (an extension of the cell membrane at the leading edge) oriented towards increasing EGF concentration (Fig. 3). Cells that were treated with antibody, on the other hand, were mostly unpolarized and had no predominant orientation, reflecting random movement. Indeed, the average CI of antibody-treated cells was lower (0.03) than control (0.21) and only 55%

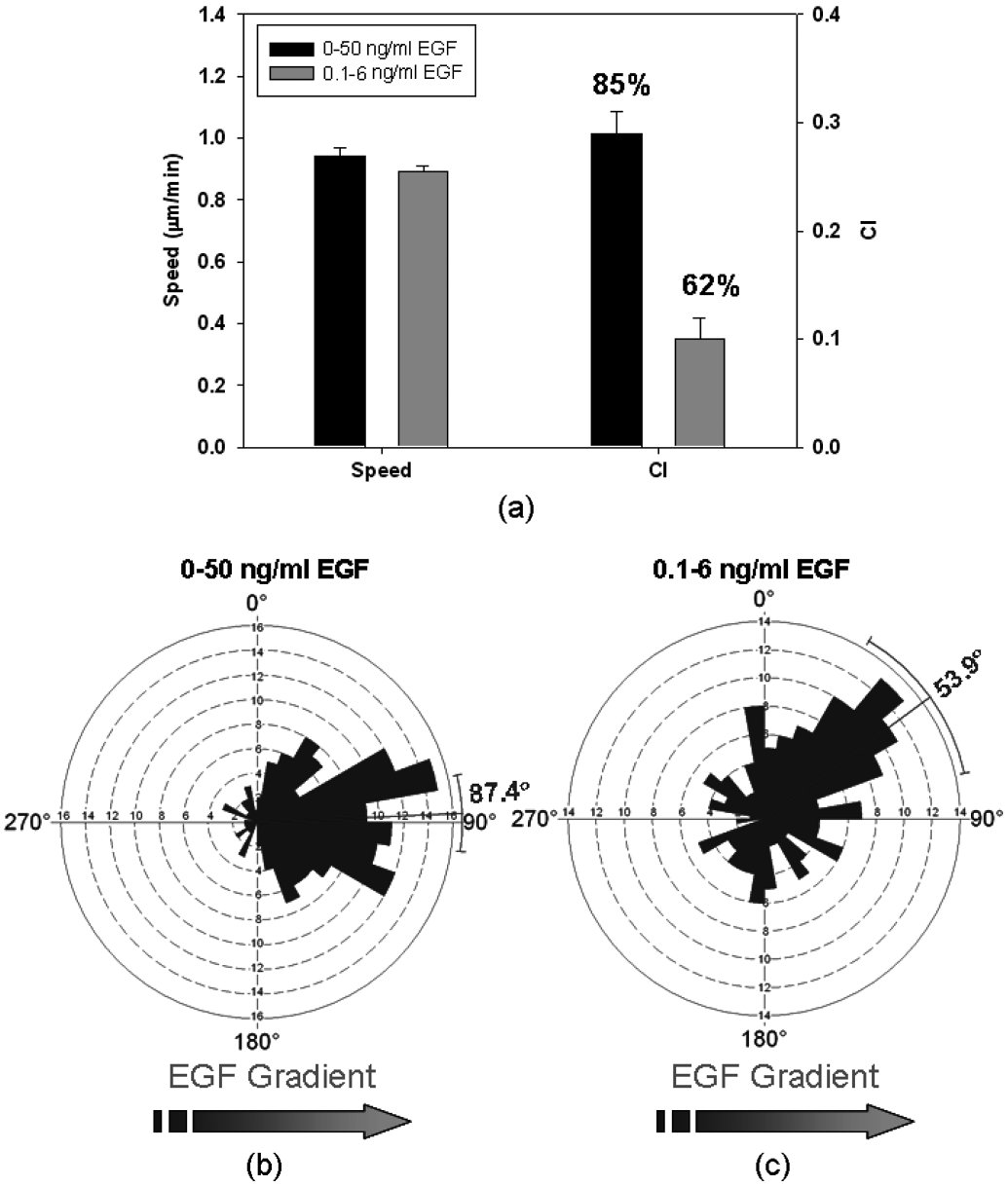

Fig. 2 Chemotactic response of MDA-MB-231 in 0–50 ng/ml and 0.1–6 ng/ml polynomial EGF gradients in parallel. (a) Average speed and chemotactic index (CI) values. Error bars represent standard error. Percentages indicate the number of cells that migrated towards the gradient. (b–c) Direction plots showing the distribution of migration angles, grouped in 10° intervals (wedges). The radius of each wedge indicates the number of cells that migrated in a particular direction. 157 cells and 170 cells were analyzed in 0−50 ng/ml and 0.1−6 ng/ml, respectively. A Rayleigh test shows that migration was directional in both ranges, with the mean angles of 87.4° and 53.9° for 0–50 ng/ml and 0.1–6 ng/ml, respectively. Arcs indicate 95% confidence intervals. In both plots, 90° is the direction of increasing EGF concentration. Cells that migrated a net distance of less than 25 μm were excluded

of cells moved towards the gradient, compared to 80% in the case of the control (Fig. 4). This was confirmed by the Rayleigh test, which showed no directional preference in the distribution of migration angles for antibody-treated cells (Fig. 4); untreated control cells exhibited a directional preference, with a mean angle of 74.8°. Again, this deviation from the gradient direction is not statistically significant, as shown by the modified Rayleigh test.

Discussion

Chemotaxis chamber design and layout

Figure 1(a) shows the design of a microfluidic gradient generator that produces a single gradient of nonlinear polynomial profile (Lin et al., 2004) (polynomial gradient from here on). The principle behind the generation and control of

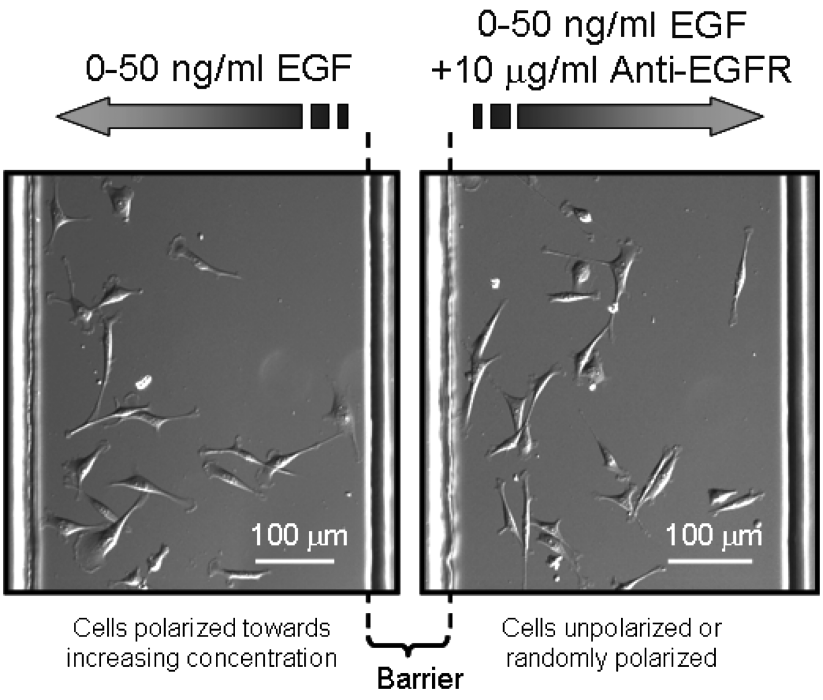

Fig. 3 DIC images of MDA-MB-231 cells treated with anti-EGFR antibody alongside untreated cells in 0–50 ng/ml EGF gradients after 3 hrs. In the absence of antibody treatment (left), most cells were polarized in the direction of increasing EGF concentration, while antibody-treated cells (right) were either unpolarized or randomly polarized

concentration gradients using microfluidics has been published elsewhere (Jeon et al., 2000; Dertinger et al., 2001). Briefly, fluid streams are repeatedly split and mixed in the gradient-generating channel network [Fig. 1(a)], the design of which determines the shape of the resulting gradient in the migration channel. For example, a network design with two inlets infused with 0% and 100% solutions yields a 0–100% linear gradient across the migration channel and perpendicular to the flow. Although the network in Fig. 1(a) has two inlets, the left inlet splits into four streams, effectively increasing the number of inlets to five. Infusing the device with media and chemoattractant-containing media into the left and right inlet, respectively, with a volumetric flow rate ratio of 4:1, produces a polynomial concentration gradient of the form:

$$C = ax^{4.2} + b$$

where C is the concentration of chemoattractant; x is the position across the migration channel; a and b are constants that depend on the width of the channel as well as the minimum and maximum chemoattractant concentrations.

Each microfluidic network generates a single microfluidic gradient; when two networks are placed in parallel and merged into one channel, two gradients are formed side by side [Fig. 1(b)]. The two polynomial gradients in Fig. 1(b) are placed opposite of each other to minimize blurring between the gradients due to diffusion. Alternatively, a physical barrier [Fig. 1(c)] can be used to avoid the blurring interface. A barrier is needed for applications that utilize small molecules (sizes < 1 kDa). Relatively large diffusion coefficients of small molecules ($D \approx 5 \times 10^{-5}$ cm^{-2}/s) allow them to quickly cross over between adjacent gradients under the flow speeds used in our experiments (4.2×10^{-2} cm/s). In addition, a barrier is needed for applications that require different pretreatments for separate group of cells. As illustrated in our example, a barrier would allow antibody-treated cells and control cells to be loaded separately while allowing side by side comparison of their migration.

EGF is a potent chemoattractant for metastatic breast cancer cells

Cancer metastasis is a complex process that involves a number of events, with multiple signals from tumor and stromal cells, the extracellular matrix, and soluble growth factors influencing the behavior of cancer cells (Levine et al., 1995; Wells, 2000; Chambers et al., 2002; Steeg, 2003). One of the most important, and best understood, growth factor systems in this regard is the EGF/EGFR system, long implicated in cancer development (Price et al., 1999; Wells et al., 2002; Steven Wiley et al., 2003). Traditionally associated with tumor cell proliferation and growth, EGFR expression has been found to correlate with the metastatic potential of various cancers (Radinsky et al., 1995; Turner et al., 1997). On the cellular level, EGF was shown to induce chemotaxis of metastatic breast cancer cells, both *in vivo* (Wyckoff et al., 2000) and *in vitro* (Bailly et al., 1998; Price et al., 1999). This is particularly relevant to metastasis, since platelets, smooth muscle cells, monocytes, and macrophages have been

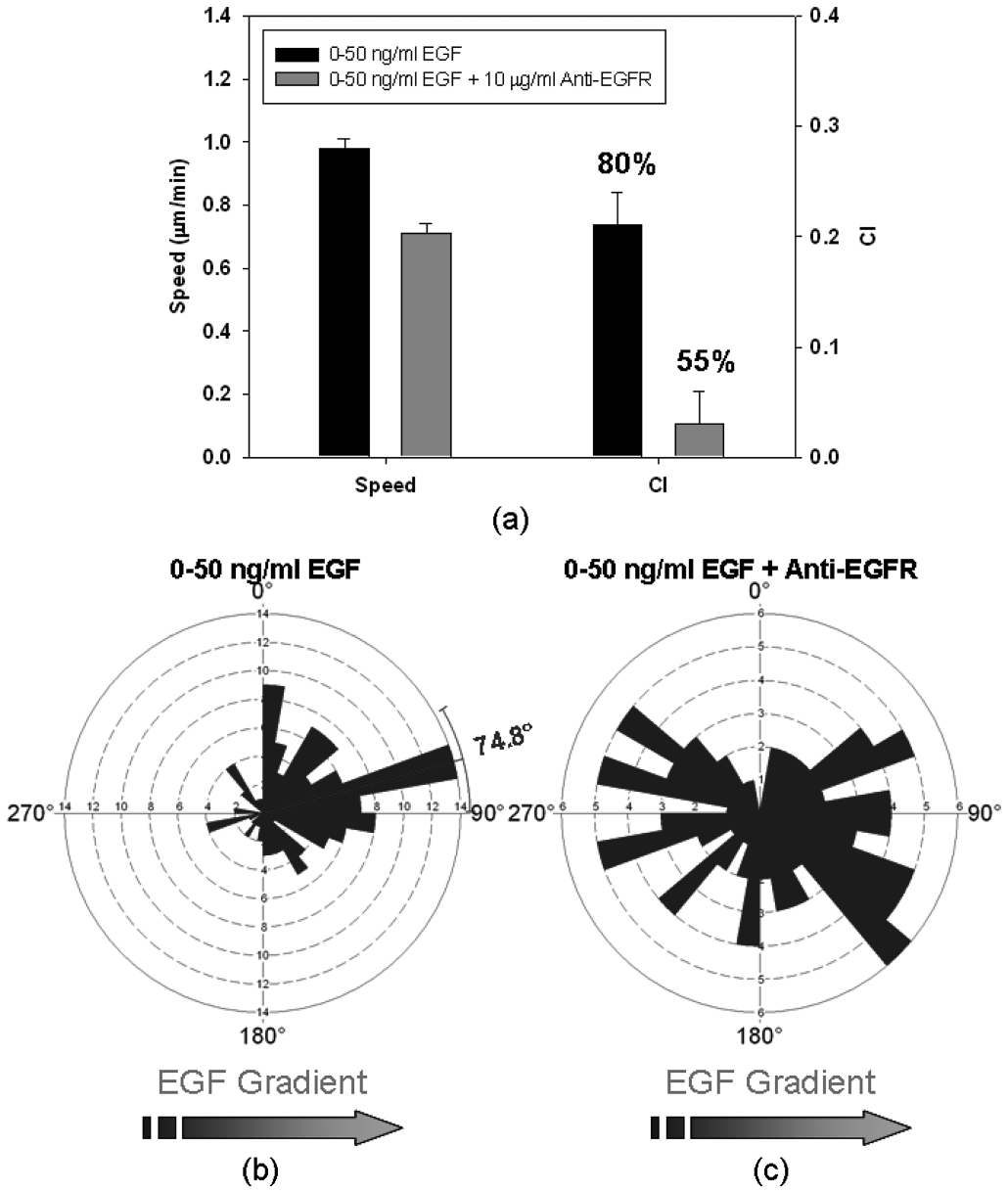

Fig. 4 Anti-EGFR antibody inhibits chemotaxis of MDA-MB-231 in a 0–50 ng/ml EGF gradient. (a) Average speed and CI for antibody-treated cells, compared with control cells side by side. Error bars represent standard error. Percentages indicate the number of cells that migrated towards the gradient. (b–c) Direction plots showing the distribution of migration angles, grouped in 10° intervals (wedges). The radius of each wedge indicates the number of cells that migrated in that direction. 123 control cells and 101 anti-EGFR treated cells were analyzed. A Rayleigh test showed that untreated cells migrated directionally, with a mean angle of 74.8° (arc indicates 95% confidence), while antibody-treated cells had no directional preference. 90° is the direction of increasing EGF concentration

shown to produce EGF along with platelet-derived growth factor (PDGF) and related growth factors (Dluz et al., 1993; Kume and Gimbrone, 1994; Peoples et al., 1995; Wyckoff et al., 2000). Gradients resulting from the release of these factors may provide chemotactic cues that direct metastatic cell motility towards blood vessels, where they can enter the blood stream and travel to other sites in the body (Wyckoff et al., 2000; Condeelis et al., 2001). In order to understand and subsequently treat metastasis, we need to understand the mechanism of cancer cell chemotaxis in response to EGF and other chemoattractants. To achieve this understanding, we must study chemotaxis in precisely controlled microenvironments, both at the single-cell level as well as the population level, in real time. This kind of detailed information cannot be obtained with conventional methods, which use macroscale diffusion. We present an example of the wealth of data that can be obtained through comparative analysis of cell migration in parallel-gradient microfluidic chemotaxis chambers.

We have previously reported that EGF gradients induce chemotaxis of the human metastatic breast cancer cell line

MDA-MB-231 (Wang et al.). Unlike other reports, we were able to define and maintain the exact mathematical form of the EGF gradient to which the cells were exposed. We showed that cells migrated chemotactically in polynomial gradients while linear gradients and uniform EGF resulted in random migration (Wang et al., 2004). This previous work demonstrated that breast cancer cells are sensitive to the profile of EGF gradient they encounter, not simply the slope of the gradient (Wang et al.). Among the polynomial EGF gradients tested (0–25 ng/ml, 0–50 ng/ml, 0–100 ng/ml), the 0–50 ng/ml gradient induced optimal directed migration. Compared to the equilibrium dissociation coefficient of EGF ($k_d = 6$ ng/ml), these gradients span concentrations that are considerably higher. The K_d can be used to model receptor binding kinetics and predict cell responses in different gradients (see Wang el al. for a brief discussion). Based on these considerations, it is necessary to investigate cell migration in gradients that are shallower in range and closer to the k_d value. Considering that growth factors may be released from macrophages or other cells around the blood vessels, the growth factor gradient would be steep, with higher concentrations near the blood vessel. Yet, the growth factor concentration would rapidly decay further away from the blood vessel, establishing a shallow gradient. Considering the widely varying gradient conditions that may exist in tissues, it is important to investigate cancer cell migration in both high-and low-range concentration gradients.

We compared the migration of breast cancer cells in a 0.1–6 ng/ml polynomial EGF gradient to a 0–50 ng/ml EGF gradient side by side (Fig. 2). The baseline of the 0.1–6 ng/ml gradient was chosen to be nonzero so that cells in the low end of the gradient would be exposed to more EGF than they would if the baseline was zero. This was done to improve the motility of cells by chemokinesis in the low growth factor region. Otherwise, cell migration in the low end of the gradient would be mostly basal. Figure 2 shows significant net movement towards the gradient in both ranges, with different efficiencies. The average CI and the percentage of cells that moved towards the gradient were lower in 0.1–6 ng/ml EGF, with a wider distribution of migration trajectories and a larger confidence interval. The average speeds in the two gradients were very close, however. This suggests that at some point between 0.1 and 6 ng/ml EGF, the receptor are being saturated, such that higher concentrations do not improve motility. Alternatively, there may be a threshold concentration that is required for inducing motility. The directional response, on the other hand, is clearly dose dependent in the ranges tested, as the shallower gradient induces a weaker response. It must be emphasized that although the mean angles in the two gradients appear to be different, neither of them significantly deviates from the gradient direction. The observed differences in migration angles are attributed to random variations in the cell population, especially since cancer cells are heterogeneous.

These data demonstrate that EGF induces chemotaxis in metastatic cells over a broad dynamic range of concentrations, and confirms its potency as a chemoattractant (Price et al., 1999). These findings may have implications for metastatic cells in the tumor microenvironment. Suppose that metastatic cells are located inside a tumor, at some distance away from a blood vessel, and that EGF is being released from a location near the blood vessel. As mentioned above, we expect the EGF concentration to be relatively high near the blood vessel but low where the metastatic cells are. Detecting a shallow concentration gradient of EGF, the metastatic cells would have a moderate chemotactic response: a fraction of the cells would migrate in the general direction of increasing EGF concentration, while the rest would wander in other directions, with the same migration speed. This behavior may actually be advantageous to the metastasizing tumor cell if we consider a scenario where multiple blood vessels are releasing growth factors, such that the metastatic cells receive conflicting signals from different directions. The fact that a certain number of cells will wander off from a given gradient direction may allow them to explore other gradient-releasing vessels, thus increasing their likelihood of reaching the blood stream and getting disseminated to other sites in the body. As the cell gets closer to a blood vessel, the EGF concentration would increase and the gradient will become steeper, resulting in strong directed migration towards the source and locking the cell in its course towards the blood vessel.

The ability to adapt to a broad range of EGF concentrations may have important implications for therapeutic efforts to treat metastasis. Several approaches are currently being employed to target the EGF/EGFR system (see the following section for more details). These efforts must be armed with a solid understanding of the dose-dependence of EGF-induced motility, such that treatments can be designed most effectively.

Effect of EGFR-blocking antibody on cancer cell migration in EGF gradient

Due to its importance in cancer, several therapeutic strategies have targeted the EGF/EGFR signaling pathway (Woodburn, 1999; Mendelsohn and Baselga, 2000). One strategy has been to use antibodies that compete with the ligands for the receptor; monoclonal antibodies against EGFR have been under development for some time (Ciardiello and Tortora, 2001; Mendelsohn, 2001). The humanized monoclonal antibody Erbitux (Cetuximab, C225) was recently approved in the US and Switzerland for the treatment of colorectal cancer. Experimentally, this antibody inhibits the growth of cancer cell lines in culture and inhibits the growth of Xenografted tumors (Fischer et al., 2003). Due to the involvement of EGF in

chemotaxis, it is important to investigate the effect of EGFR antibodies on cancer cell migration and chemotaxis.

Using the parallel gradient chamber [Fig. 1(c)], we examined the effect of anti-EGFR treatment on the migration of metastatic breast cancer cells alongside untreated control cells. Antibody treatment abolished the chemotactic response of the cancer cells and resulted in random migration. This is clearly seen in the morphology of antibody-treated cells (Fig. 3), which were mostly unpolarized. Untreated cells, on the other hand, had well defined lamellipodia that were oriented towards increasing EGF concentration. This polarization is characteristic of cells undergoing chemotaxis (Wyckoff et al., 1998; Condeelis et al., 2001). Moreover, antibody-treated cells had a very low average CI, and a uniform distribution of trajectories (Fig. 4), while control cells had significant clustering of trajectories in the gradient direction.

Others have previously demonstrated the inhibition of EGF-induced chemotaxis of MDA-MB-231 cells using anti-EGFR antibody in Boyden chambers (Price et al., 1999). Since the Boyden chamber is an end-point assay, random motility and directed motility cannot be visually distinguished. A series of conditions with different chemoattractant concentrations must be compared and evaluated using a checkerboard analysis in order to distinguish chemotaxis from chemokinesis. Consequently, the effect of antibody treatment can only be evaluated in regards to chemotaxis as a whole, not knowing if the antibody is interfering with motility, directional sensing, or both. The microfluidic chemotaxis chamber allows the migration process to be examined in real time, providing details of individual cell trajectories as well as distributions of cell populations. We can thus evaluate both motility and directionality independent of each other. With this capability, we found that the anti-EGFR antibody targets both motility and directional sensing: in the presence of anti-EGFR, cells moved randomly with speeds similar to those at basal levels (non-EGF stimulated, data not shown). This verifies that the observed migratory response occurs specifically via EGFR, and that blockade of this receptor does not affect basal migration.

This approach can be used to categorize different types of inhibitors based on their mechanism of action. Antibodies act at the receptor level and block all the downstream signaling associated with the receptor, thus inhibiting the entire chemotactic response. Inhibitors that act further downstream may only block certain aspects of the chemotactic response, leaving the rest of the process intact. The mechanism of action of the inhibitor could be used as a measure of its effectiveness in metastasis therapy. One can envision a situation where a chemoattractant is specifically associated with cancer cell metastasis, and does not influence other cells. In such a case, inhibitors that completely block chemotaxis may be more effective, and may result in the best therapeutic outcome.

On the other hand, inhibiting only one aspect of chemotaxis may be desirable in certain cases. For example, it has been proposed that growth factor-induced migration is necessary for cancer cell invasion, but that adhesion-mediated basal migration is sufficient for normal cell function (Wells et al., 2002). Evidence suggests that inhibition of PLCγ, a signaling molecule downstream of certain growth factor receptors, blocks growth factor-induced motility but leaves basal motility intact (Turner et al., 1997; Kassis et al., 2001). This would provide a therapeutic window, allowing metastatic cell migration to be targeted without interfering with normal processes. Using the microfluidic chemotaxis chamber, the effects of different inhibitors can be investigated in a quantitative manner, allowing comparisons of effectiveness based on quantitative data, in addition to qualitative observations.

Conclusion

We have developed a parallel-gradient microfluidic chemotaxis chamber capable of generating different experimental conditions in parallel, allowing individual cells to be investigated in detail while providing quantitative, statistically meaningful data for the whole cell population. Traditionally, drug candidates are evaluated in terms of their effects on proliferation using cell-based assays in microtiter plates. The microfluidic chemotaxis chamber described here represents a platform to investigate the effects of pharmaceutical compounds on cell migration (in terms of speed, chemotactic index, and directional orientation) and provides a means to evaluate their effectiveness in relation to metastasis. Coupled with conventional cell based assays, this approach may provide information about the different pathways involved in the migration of cancer cells, how they are modulated, and if there is any cross-talk between pathways. This knowledge may result in novel approaches for treatment of metastasis that target cell motility.

Acknowledgments This research is supported by the Whitaker Foundation, Concern Foundation (Grant No. CFCR-30575), and the Department of Defense (Grants No. DAMD17-03-1-0515 and No. DAMD17-03-1-0673).

References

M. Bailly, L. Yan, G.M. Whitesides, J.S. Condeelis and J.E. Segall, Experimental Cell Research **241**, 285–299 (1998).
C.G. Bredin, Z. Liu, D. Hauzenberger and J. Klominek, Int J Cancer **82**, 338–45 (1999).
A.F. Chambers, A.C. Groom and I.C. MacDonald, Nat Rev Cancer **2**, 563–72 (2002).
F. Ciardiello and G. Tortora, Clin Cancer Res **7**, 2958–2970 (2001).

J.S. Condeelis, J.B. Wyckoff, M. Bailly, R. Pestell, D. Lawrence, J. Backer and J.E. Segall, Semin Cancer Biol **11**, 119–8 (2001).
S.K.W. Dertinger, D.T. Chiu, N.L. Jeon and G.M. Whitesides, Anal Chem **73**, 1240–1246 (2001).
S. Dluz, S. Higashiyama, D. Damm, J. Abraham and M. Klagsbrun, J Biol Chem **268**, 18330–18334 (1993).
O.M. Fischer, S. Streit, S. Hart and A. Ullrich, Current Opinion in Chemical Biology **7**, 490–495 (2003).
N.L. Jeon, H. Baskaran, S.K.W. Dertinger, G.M. Whitesides, L. Van De Water and M. Toner, Nat Biotechnol **20** 826–830 (2002).
N.L. Jeon, S.K.W. Dertinger, D.T. Chiu and G.M. Whitesides, Langmuir **16**, 8311–8316 (2000).
J. Kassis, D.A. Lauffenburger, T. Turner and A. Wells, Seminars in Cancer Biology **11**, 105–119 (2001).
N. Kume and M.J. Gimbrone, J Clin Invest **93**, 907–11 (1994).
M.D. Levine, L.A. Liotta and M.L. Stracke, EXS **74**, 157–179 (1995).
F. Lin, W. Saadi, S.W. Rhee, S.-J. Wang, S. Mittal and N.L. Jeon, Lab Chip **4**, DOI: 10.1039/b313600k (2004).
G. Maheshwari, A. Wells, L.G. Griffith and D.A. Lauffenburger, Biophys J **76**, 2814–23 (1999).
J. Mendelsohn, Endocr Relat Cancer **8**, 3–9 (2001).
J. Mendelsohn and J. Baselga, Oncogene **19**, 6550–65 (2000).
G. Peoples, S. Blotnick, K. Takahashi, M. Freeman, M. Klagsbrun and T. Eberlein, PNAS **92**, 6547–6551 (1995).
J.T. Price, T. Tiganis, A. Agarwal, D. Djakiew and E.W. Thompson, Cancer Research **59**, 5475–5478 (1999).
R. Radinsky, S. Risin, D. Fan, Z. Dong, D. Bielenberg, C. Bucana and I.J. Fidler, Clin Cancer Res **1**, 19–31 (1995).
P.S. Steeg, Nat Rev Cancer **3**, 55–63 (2003).
H. Steven Wiley, S.Y. Shvartsman and D.A. Lauffenburger, Trends in Cell Biology **13**, 43-50 (2003).
T. Turner, M.V. Epps-Fung, J. Kassis and A. Wells, Clin Cancer Res **3**, 2275–82 (1997).
S.-J. Wang, W. Saadi, F. Lin, C.M.-C. Nguyen and N.L. Jeon, Exp Cell Res **300**, 180–189 (2004).
A. Wells, Adv Cancer Res **78**, 31–101 (2000).
A. Wells, J. Kassis, J. Solava, T. Turner and D.A. Lauffenburger, Acta Oncol **41**, 124–30 (2002).
G.M. Whitesides, E. Ostuni, S. Takayama, X. Jiang and D.E. Ingber, Annu Rev Biomed Eng **3**, 335–73 (2001).
P.C. Wilkinson, Journal of Immunological Methods **216**, 139–153 (1998).
J. Woodburn, Pharmacol Ther **82**, 241–50 (1999).
J.B. Wyckoff, L. Insel, K. Khazaie, R.B. Lichtner, J.S. Condeelis and J.E. Segall, Experimental Cell Research **242**, 100–109 (1998).
J.B. Wyckoff, J.G. Jones, J.S. Condeelis and J.E. Segall, Cancer Res **60**, 2504–2511 (2000).
J.B. Wyckoff, J.E. Segall and J.S. Condeelis, Cancer Res **60**, 5401–4 (2000).
X. Yang, J. Corvalan, P. Wang, C. Roy and C. Davis, J Leukoc Biol **66**, 401–410 (1999).
J.H. Zar, Biostatistical Analysis (Prentice-Hall, Inc, Upper Saddle River, New Jersey, (1996)